# ⓒⓘ🄎⊜ CC BY-NC-ND 4.0

## You are free to:

**Share** — copy and redistribute the material in any medium or format

The licensor cannot revoke these freedoms as long as you follow the license terms.

## Under the following terms:

**Attribution** — You must give appropriate credit , provide a link to the license, and indicate if changes were made . You may do so in any reasonable manner, but not in any way that suggests the licensor endorses you or your use.

**NonCommercial** — You may not use the material for commercial purposes .

**NoDerivatives** — If you remix, transform, or build upon the material, you may not distribute the modified material.

**No additional restrictions** — You may not apply legal terms or technological measures that legally restrict others from doing anything the license permits.

## Notices:

You do not have to comply with the license for elements of the material in the public domain or where your use is permitted by an applicable exception or limitation .

No warranties are given. The license may not give you all of the permissions necessary for your intended use. For example, other rights such as publicity, privacy, or moral rights may limit how you use the material.

# Probing the correlation between morphology and optical anisotropy in ZnTPP films grown at different temperatures

Rossella Yivlialin [*], Lorenzo Ferraro , Claudia Filoni , Isheta Majumdar , Alberto Calloni ,
Francesco Goto , Marco Finazzi , Lamberto Duò , Franco Ciccacci , Gianlorenzo Bussetti

*Department of Physics, Politecnico di Milano, 20133 Milan, Italy*

ABSTRACT

Films of tetraphenylporphyrins (TPP) have been recently investigated for their ability in protecting graphite electrode surfaces from degradation. The effectiveness of the protection depends on both the molecule-substrate and molecule–molecule interactions, which determine the type of film growth and its morphology. For instance, meso-tetraphenyl porphyrin-Zn(II) (ZnTPP) arranges differently depending on the substrate, conditions used for deposition and post-growth treatments. Since many parameters influence film morphology and strategies to reach an efficient protective coverage, here we investigate the role of the substrate temperature in determining morphological variations in thick ZnTPP films. ZnTPP molecules were sublimated by an organic molecular beam epitaxy (OMBE) system on a highly oriented pyrolytic graphite (HOPG) substrate, controlled in temperature by a variable temperature cryostat. The film morphology was characterized by atomic force microscopy (AFM), whereas the type of growth by reflectance anisotropy spectroscopy (RAS), which is highly sensitive to the orientation and type of arrangement of molecules on the substrate; changes in the film valence electronic structure were monitored *in situ* by UV photoemission spectroscopy (UPS). The comparison between AFM and RAS investigations clearly correlates a ZnTPP film morphology to the characteristic optical signal, both influenced by temperature conditions and diffusivity of molecules on the substrate.

## 1. Introduction

Nowadays, there is a strong demand for simple and efficient strategies to protect electrodes from degradation caused by different reasons. In fact, many of the most used electrode materials, such as lithium-containing metal oxide or positive electrode materials in general, suffer different issues of instability and structural damage, which result in a severe attenuation of capacity and a poor rate performance [1,2]. The degradation is mainly caused by the detrimental interfacial reaction between the material and the electrolyte solution, which can be induced simply by a direct contact or by the application of high voltages. Related to this, another reason for degradation is attributed to irreversible side reactions, which typically affect and limit the cycle life of energy storage devices, such as lead-acid and lithium-ion batteries [3,4]. To solve the issue of degradation, carbon materials (such as graphite, graphene, carbon black, carbon nanotubes) have been widely applied in energy storage and conversion, as an effective way to protect the electrodes [5] but also improve their electrochemical performance, owing to favorable

chemical/electrochemical stability and conductivity of carbon materials [6,7]. However, the use of carbon-based electrodes is not always beneficial [8,9]; an example of this is represented by graphite, which is known to undergo structural and morphological damages (*i. e.*, carbon dissolution and formation of bumps called "blisters" [10]) in acidic electrolytes (*e. g.*, diluted $H_2SO_4$, $HClO_4$ and $H_3PO_4$), even under electrochemical (EC) potentials way lower than typical working potential ranges in batteries [11–13]. Although the impact of an altered graphite on the performance of devices has not been directly demonstrated yet, there is no doubt about the need of modifying the electrode/electrolyte interface, in order to protect the graphite surface from side effects of the EC reactions in water-based acidic solutions.

Among several engineering technologies that exist for modifying the graphite/electrolyte interface (*e. g.*, the atomic layer deposition of metal oxides [14]), vacuum layer-deposition of organic molecules has focused the attention of the scientific community in the last decade, because of the low costs, tuneability and stability of the materials [15]. More specifically, vacuum-deposited films of porphyrin molecules [such as free-

base tetraphenyl porphyrin (H$_2$TPP) and meso-tetra(3,5-di-*tert*-butyl-phenyl)porphyrin (H$_2$TBP) [16]] show a promising attitude in protecting the graphite electrode surface from carbon dissolution and blistering phenomena caused by the EC anion-intercalation, without affecting the characteristic EC properties of the electrode [17,18]. However, some strategies are required to improve the potency and durability of these organic layers. For instance, it is possible to tune the properties of the layers by changing the composition and structure of the molecules [16], or explore different morphologies of the organic layers by changing deposition and growth conditions, in order to find the most efficient coating. Regarding to this, the effect of deposition temperature on the growth of heteroepitaxial inorganic/organic films has attracted great interest, especially modelling the main mechanisms that control and determine the film morphology observed experimentally, to design the most suitable conditions to obtain materials with the desired features [19]. Within this context, in the present work we explore the correlation between morphology (investigated by atomic force microscopy, AFM) and optical anisotropy of vacuum-deposited zinc tetraphenyl porphyrin (ZnTPP) films, grown on a highly oriented pyrolytic graphite (HOPG) substrate, kept at different temperatures (*T*) during film deposition. The use of a reflectance anisotropy spectroscopy (RAS) to measure the optical anisotropy signal of the "as-prepared" ZnTPP films is motivated by the high sensitivity of this technique (down to signals lower than $10^{-4}$ [20]) to molecular aggregates and assembled molecular layers [21,22]; in particular, the use of polarized light offers the opportunity to study systems that exhibit anisotropies due to electronic or morphological characteristics of the organic layer grown onto an isotropic substrate (which is the case of HOPG). By harnessing the correlation between AFM and RAS measurements, we established a unique relationship between film morphology and optical signal; one of the advantages of this is that the monitoring of changes in the only optical signal can be used to identify potential degradation processes affecting the film morphology in extreme or life shortening environmental conditions (*e. g.*, far-from-equilibrium conditions [23], electrochemical oxidation conditions), where the monitoring by AFM or other microscopy techniques would be strongly constrained.

As an additional check, the preservation of the valence electronic structure of the molecular films after each deposition was verified by measuring the valence band of the samples, by using UV photoemission spectroscopy (UPS).

## 2. Experimental

### 2.1. Experimental set-up and methods

The experimental apparatus consists in a multi-chamber ultra-high vacuum (UHV) system (base pressure in the low $10^{-8}$ Pa range) described in detail elsewhere [24], coupled to a chamber for organic molecular beam epitaxy (OMBE) [25]. The OMBE deposition system hosts four Kundsen cells, with a sample-to-crucible distance of about 10 cm (no flux liners are used). Temperature controllers stabilize the crucibles temperature within 0.5 °C. One of the cells is filled with ZnTPP molecules, provided by Sigma Aldrich and purified in vacuum. Molecules purification was achieved by heating the porphyrin powder in the OMBE chamber up to 180 °C. Upon heating, the pressure initially increases by several orders of magnitude: the process was carried on for few days, until the OMBE base pressure ($5 \times 10^{-8}$ Pa) was fully recovered. Porphyrin sublimation was then performed in the low $10^{-6}$ Pa range. A quartz microbalance (QM) is used to calibrate the molecular beam flux at the sample deposition site. Substrate temperatures in the −115–130 °C range were attained on a deposition stage in thermal contact with a LN$_2$ reservoir and equipped with an ohmic heater. A temperature controller connected with the heating element was used to set the substrate temperature with an overall accuracy better than 2 °C. The deposition stage was calibrated by attaching a K-type thermocouple directly on the sample holder. Photoemission spectroscopy is performed

by exciting electrons out of the sample at normal emission with UV radiation (He I, h$\nu$ = 21.2 eV), and detecting them by means of a 150 mm hemispherical analyzer (SPECS GmbH) [24]. The full width at half-maximum (FWHM) energy resolution was set to 50 meV for UV photoemission spectroscopy. Photoelectron spectroscopy experiments were performed under conditions of no charging effects in the molecular film.

A high-sensitivity home-made RAS apparatus [20], with a light spot diameter of about 5 mm, was used to collect the optical spectra. The light coming from a Xe arc lamp is linearly polarized ($\alpha$-direction) by a Glan-Thomson optical system and passes through a Photo-elastic Modulator (PEM), which rotates the light polarization along two mutually orthogonal directions ($\alpha$ and $\beta$) at a double frequency with respect to the resonance frequency of 50 kHz. The light beam is properly focused on the sample by a system of lenses and reflected within an angle of few degrees. Along the reflected light-path, after a second system of lenses, a second Glan polarizer (called analyzer) linearly polarizes the light coming from the sample; follows a monochromator and then a photomultiplier detector.

Experimentally, the RAS signal is defined as the difference in the reflectivity between $\alpha$ and $\beta$ directions ($R_\alpha$, $R_\beta$) normalized by the mean total reflectivity ($\overline{R}$):

$$\frac{\Delta R}{\overline{R}} = 2\frac{R_\alpha(\omega) - R_\beta(\omega)}{R_\alpha(\omega) + R_\beta(\omega)} \tag{1}$$

While the mean sample reflectivity ($\overline{R}$) can be measured by a simple multimeter, the sample anisotropy ($\Delta R$) is detected by a phase-sensitive lock-in amplifier, which measures a signal proportional to $\Delta R = R_\alpha - R_\beta$ at a double frequency (namely, 100 kHz) with respect to the PEM resonance frequency.

In the case of thin organic layers, the alignment of the sample with respect to the $\alpha$ and $\beta$ directions of PEM is a priori unknown; an azimuthal analysis is thus required to find the maximum of the RAS signal. For the molecular samples analyzed in this work, the maximum value of the anisotropy (in modulus) is generally reached when the direction of graphite exfoliation is aligned along the $\alpha$ or $\beta$ direction (within 10°) [26,27]. RAS spectra were collected in the 330–650 nm wavelength ($\lambda$) range, with a step of 2 nm; however, to focus the discussion on the main porphyrin optical transition, only a shorter wavelength range centered on the Soret-band (*i. e.*, 400–500 nm) is reported in the text.

AFM characterizations were performed by using a commercial scanning probe microscope (5500 by Keysight Technology). The images were acquired in tapping-mode and in attractive regime, with silicon tips from Bruker (cantilever force constant: 2.8 N/m; $\nu_0$ = 75 kHz); typical scan rates of about 1 Hz were used.

### 2.2. Sample preparation

Samples consist in films with a nominal thickness of 6 nm (*i. e.*, about 20 ML, with 1 ML = 3.06 Å) of ZnTPP molecules (Scheme 1) to avoid electronic interactions with the substrate [25]. The organic films were deposited in vacuum on highly oriented pyrolytic graphite (HOPG, by Optigraph GmbH, with a mosaic spread of 0.4° to ensure a high reflectivity useful for the optical spectroscopy characterization). Before each molecular deposition, HOPG was exfoliated by using an adhesive tape always along the same direction, to create a preferential orientation for the HOPG steps, thus orienting the porphyrin growth and ensuring a special direction for the alignment of the RAS apparatus.

The films were grown in OMBE chamber; the sublimation rate was kept at 1 Å/min, corresponding to a sublimation temperature in the range 270–285 °C. The substrate was exposed to the calibrated molecular flux once the deposition stage had reached the desired temperature setpoint.
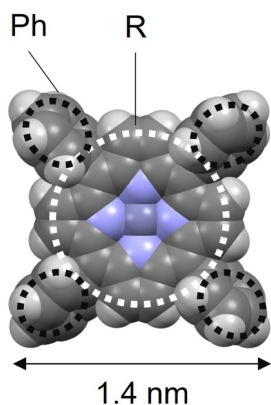
**Scheme 1.** Structure of the ZnTPP molecule: dark grey balls = C-atoms; light grey balls = H-atoms; light violet balls = N-atoms; dark violet ball (in the center of the molecule) = Zn-atom. For the sake of clarity, labels indicating the tetrapyrrolic ring (R) and one of the four phenyl groups (Ph) are reported. The average molecular size is indicated at bottom.

## 3. Results and discussion

In Fig. 1a, the morphology of the ZnTPP film grown onto the HOPG substrate at RT is showed. In these experimental conditions, molecules arrange onto the HOPG substrate by following a Stransky-Krastanov growth, in which a flat 2D wetting layer is first formed and then covered by regular 3D islands, with typical long-side size of 300–500 nm and height of 10–20 nm. The cross-sectional profile, reported below the image, reveals the characteristic sharp edges, placed to form angles of about 90°, of the ZnTPP 3D islands (i. e., crystallites). On ZnTPP crystallites grown in similar experimental conditions, X-ray/electron diffraction (XRD/TEM) measurements revealed the coexistence of two polymorphs, with a tetragonal symmetry (*l4/m*) of crystal structure [23,28].

Statistically, ZnTPP crystallites cover about 60 % of the HOPG surface, and, only in correspondence of graphite edges or limited terraces (high step distribution), they show reduced sizes of about 70 –100 nm.

The reflectance anisotropy (RA) signal of the sample is showed by the

RA spectrum reported in panel b. The maximum value of anisotropy, with an intensity of about 0.8 %, is placed at $\lambda$ = 420 nm, within the spectral range of the main absorption band of the ZnTPP molecule (i. e., the Soret-band). In this respect, the optical anisotropy as measured by RAS can be interpreted by using the so-called "three-layer" model, in which the substrate, the organic layer and the environment are described as distinct phases, characterized by specific dielectric functions. In the limit of layer thickness smaller than the excitation wavelength and above the gap of the substrate, the RA signal is seen as the sum of the dispersive and absorptive parts of the porphyrin layer dielectric function, weighted by characteristic functions of the substrate (HOPG, in our case). In the event of multi-layer organic coverages, as in our experiments, the interpretation of the RA spectrum is not trivial, due to different optical contributions coming from the substrate and the complex stratified structure of the organic film. However, we note that in spectrum of Fig. 1, the line-shape resembles those ones reported in Refs. [22,29], where the so called "derivative-like" shape (consisting in the difference between two Soret-transitions with two different widths, one for each direction of the polarized excitation) was observed in the case of self-assembled multilayered samples of porphyrins (such as Langmuir-Blodgett films). In that case, the excitation of each molecule was modeled by a harmonic oscillator dipole moment that responds to local electric field, which includes the external electric field and the molecules-induced field. It was demonstrated that the RA signal strongly depends on the orientation of the dipoles in any given layer, in particular, on the twisting and tilting angles of the dipoles in relation to the substrate: in more superficial layers, the interaction of molecules with the substrate is screened by the underlying layers, so that the molecules tend to straighten up. It was observed that the variation of molecule orientation leads to an evolution of the RA spectrum from peak-like (i. e., proportional to the Soret-band), in the case of low molecular coverages, to derivative-like, as the thickness of the coverage increases [22]. Since the high molecular coverage of our samples, we reasonably assume a similar explanation for the line-shape of RA spectrum in Fig. 1, where the derivative-like shape arises from the superimposition of different optical contributions generated by the porphyrin multi-layer.

As a side note, we mention the observation of a shoulder at a lower wavelength (about $\lambda$ = 375 nm), in a spectral range consistent with that one of the vibronic features in ZnTPP absorption spectra [30].

In Fig. 2, data of the three most representative samples are shown. In panel a, the morphology of the organic layer grown onto HOPG kept at *T* = − 75 °C reveals a uniform covering of terraces and steps (these latter clearly visible in the cross-sectional profile below the image), producing a root mean square roughness (Sq) of about 0.7 nm, compared to less than 0.35 nm of the bare HOPG surface. Interestingly, very few and small crystals are visible on the film.

The RA spectrum (panel b) shows a weak feature (of about 0.1 % of intensity) in the Soret-band region, as we would expect in case of a relatively thick film where molecules can arrange on the sample surface owning different tilt-angles, as the film thickness increases [22]. This strongly indicates that, differently than at RT, at very low *T*, the kinetic energy of ZnTPP molecules is such that the formation of a uniform coverage of the HOPG surface, with very few and isolated crystallites, and a random orientation of molecules, is favored.

It is worth to mention that, with substrate at *T* = 0 °C, the ZnTPP film exhibits a Stransky-Krastanov growth, with narrow (i. e., with lateral sizes of about 100 nm) and sharp 3D islands, with heights comparable to the ones of the islands observed after the growth at RT. In this case, the optical anisotropy signal is well pronounced, reaching an intensity of about 1 % (see Fig. 1 in the Supporting Information).

Another interesting case is represented by the sample grown on the substrate at *T* = 105 °C (see panel c). The behavior of this sample is very different from the one in panel a. The topography image shows a highly dense coverage of wide and flat ZnTPP crystallites (for the sake of clarity, see Fig. 2a,b of the Supporting Information), with lateral sizes of more than 2 μm and heights of 20 nm. The observation of wider and
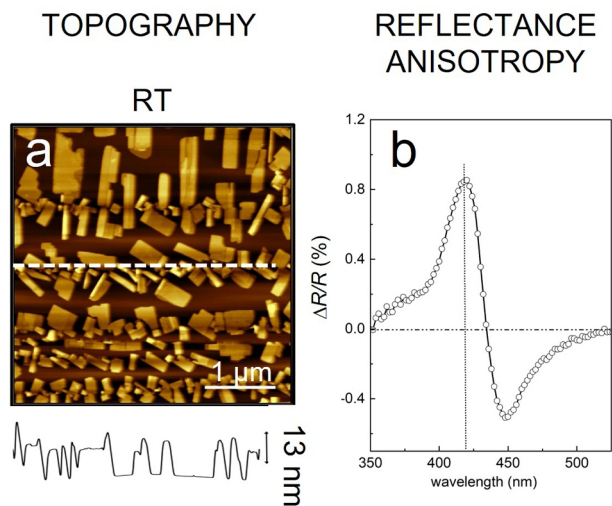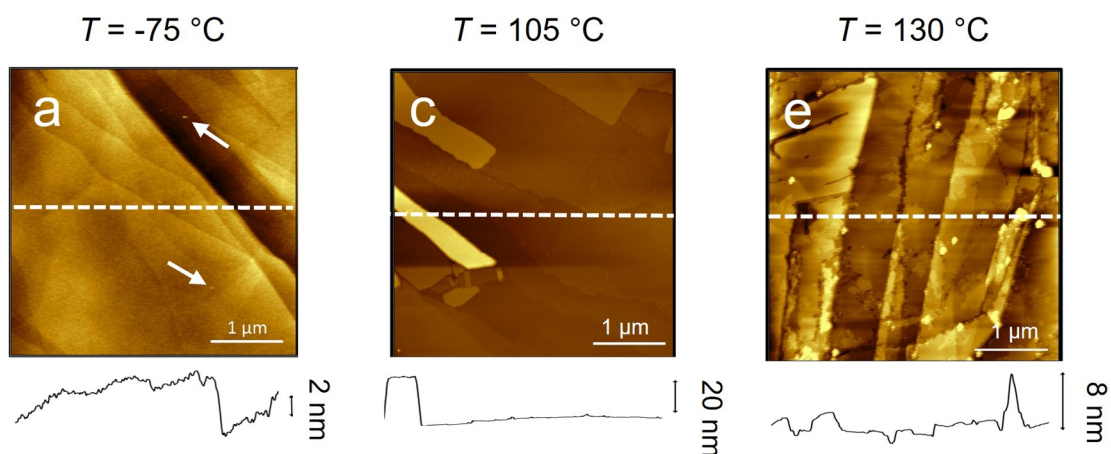


**Fig. 1. a)** Topography image [(5 × 5) μm$^2$] of a 6 nm-thick film of ZnTPP grown onto an HOPG substrate kept at RT. White arrows indicate some of the step edges on the HOPG surface. The cross-section profile is taken along the white dash line and reported below the image. **b)** Reflectance anisotropy spectrum acquired *ex situ* on the sample. Straight lines are placed in correspondence, respectively, of the position of the main peak (dot line) and of the zero signal (dash-dot-dot line).

# TOPOGRAPHY

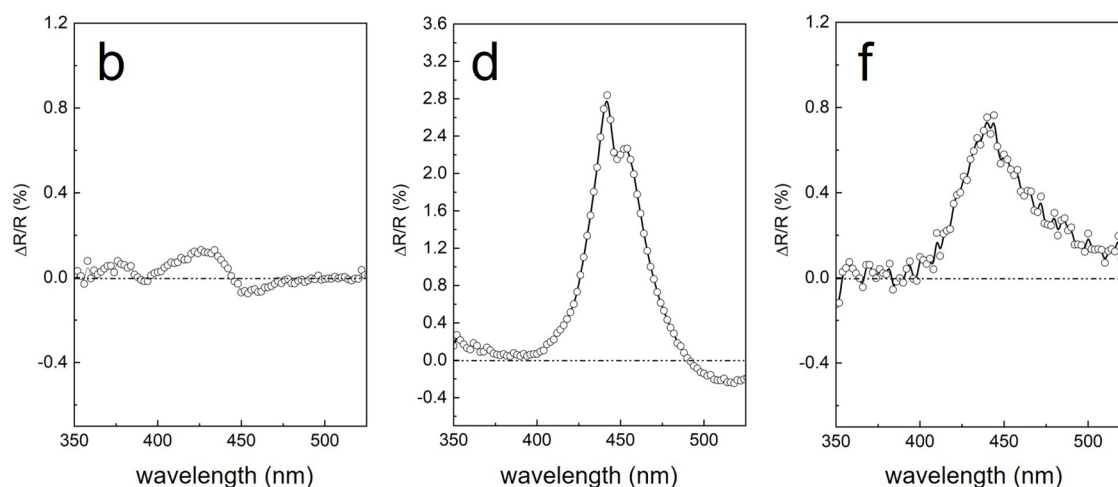$T = -75\ °C$      $T = 105\ °C$      $T = 130\ °C$



# REFLECTANCE ANISOTROPY



**Fig. 2.** Topography images [(4 × 4) μm²] of a 6 nm-thick film of ZnTPP grown onto the HOPG substrate kept at **a)** $T = -75\ °C$; **c)** $T = 105\ °C$; **e)** $T = 130\ °C$. The cross-section profile is taken along the white dash line and is reported below each image. White arrows in panel **a** indicate tiny ZnTPP crystallites. In panels **b**, **d**, **f** RA spectra acquired *ex situ* on samples showed, respectively, in panel **a**, **c** and **e**, are reported.

taller 3D islands in this case could be a consequence of a large mobility of the molecules at this temperature, which allows the molecules to reach the island borders and move to their tops. For this reason, the ZnTPP crystallites get taller as the $T$ increases [19].

The optical anisotropy spectrum (panel d) shows a very complex line-shape, more peak-like than derivative-like, with two peaks: the first one centered at $\lambda = 442$ nm, and the second one at $\lambda = 454$ nm, both red-shifted with respect to the peak showed in panel b; in addition, the vibronic feature is not clearly distinguishable.

Beyond the complexity of the spectrum, we note that, among all the measured samples, here the intensity of the signal reaches the maximum value of about 2.8 % (see also Fig. 3 of the Supporting Information). In this respect, we speculate that at $T$ higher than 50°C, the kinetic energy of ZnTPP molecules is high enough to favor the diffusion of molecules towards the step edges of the HOPG substrate, these latter inducing a preferential alignment of the ZnTPP crystallites and the maximization of the optical anisotropy. In addition, the peak-like line-shape of the spectrum could suggest that molecules tend of lying flat-on the substrate, to form, at this $T$, new crystal polymorphs which maximize the surface-volume ratio of the organic coating.

In Fig. 2e, we observe the morphology of the ZnTPP film grown on the HOPG substrate at $T = 130\ °C$. Here, the organic film looks clearly damaged. By looking at both topography image and cross-sectional profile, we observe that ZnTPP crystallites do not show the same sharp and regular edges observed in Figs. 1 and 2c; instead, crystals are characterized by irregular jagged edges and mean heights inferior to those previously discussed (*i. e.*, less than 3 nm). The RA spectrum (panel f) is remarkably consistent with the morphological information obtained by the AFM investigation and shows a reduced intensity (less than 0.8 %) of the optical anisotropy with respect to the sample grown at $T = 105\ °C$, implying a reduction also of the level of alignment of ZnTPP crystallites along the step edges. Interestingly, we find that some similarities of the line-shape with the spectrum reported in Fig. 2d, in terms of spectral composition and peak positions. However, a further investigation of the optical signal requires a quantitative theoretical analysis that is beyond the purpose of this work.

In Fig. 3, the photoemission spectra of the valence band of the samples grown on the HOPG substrate at different $T$ (see labels on the right side of the spectra) are reported.

Notwithstanding the variability observed in the morphology and optical response of the films grown at different temperatures, all the spectra show approximatively the same line-shape, in turns
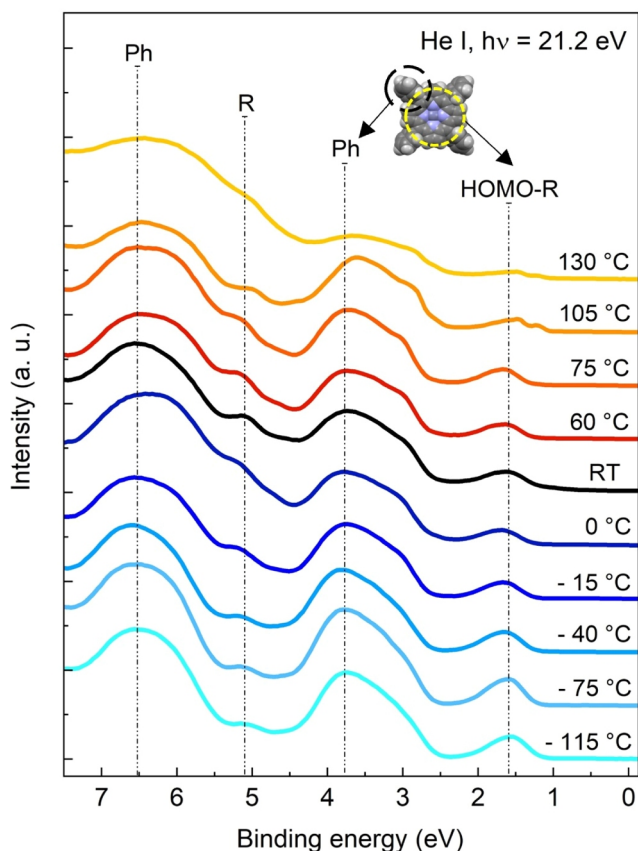
**Fig. 3.** Valence band photoemission spectra collected at He I photon energy (21.2 eV) on 6 nm-thick ZnTPP films, grown on the HOPG substrate kept at different *T* (see labels reported on the right side). On top, labels indicating the assignment of the main spectroscopic features to photoemission from the main molecular ring (-R) and phenyl groups (Ph). See the ZnTPP molecule schematics and the text for further details.

characteristic of weakly interacting ZnTPP molecules, as is the case of porphyrin multi-layers, where Van der Waals forces dominate the intermolecular interactions (see, for instance, the spectroscopic results obtained in Ref [25] for nm-thick films). The feature at about 1.6 eV is assigned to photoemission from the highest occupied molecular orbitals (HOMO) of the molecule, localized on the tetrapyrrolic ring (-R), while the feature at about 3.8 eV can be assigned to levels localized on the phenyl groups (Ph) [25,31]. At binding energies between 4.5 and 7.5 eV, other two features assigned, respectively, to R-levels (at about 5.1 eV) and Ph-levels (at about 6.5 eV) are visible [31]. Deviations from this picture are observed only at the highest temperature explored (105 and 130 °C), where the spectra show a slightly more complex line-shape (see, *e. g.* the HOMO –R feature) and then also a general broadening of the photoemission features. This is possibly related to more radical changes in the film structure, affecting also the electronic interactions. Overall, however, the presented UPS results return a picture where the molecular layers retain their electronic characteristics within a large range of different morphologies, making this technique truly complementary to both microscopy and optical anisotropy.

## 4. Conclusion

In the present work, we showed how the temperature of substrate strongly influences the growth kinetics of vacuum deposited ZnTPP films on a HOPG surface. A different diffusivity of molecules on the surface, caused by a variation of both the molecule –substrate and molecule–molecule interactions with the temperature, results in a significant modification of the morphological and optical properties of the

molecular films. In the specific, we showed that at very low *T* (*i. e.*, about −75 °C), where the diffusivity tends to zero, ZnTPP molecules uniformly cover the HOPG terraces. Because of the high symmetry of HOPG, molecules deposit on the flat terraces by following random orientations, which result in the formation of an almost optically isotropic organic film. As the *T* of substrate increases, the diffusivity of molecules on the surface also increases, and molecules can reach the step edges present on the HOPG substrate. Step edges, by breaking the symmetry of the surface, induce a preferential orientation of the molecular crystal nucleation (*i. e.*, heterogeneous nucleation regime), favoring the formation of ZnTPP crystallites aligned along the HOPG steps, which are orthogonal to the exfoliation direction of HOPG. This leads the organic film to show a pronounced optical anisotropy, with a maximum value observed in correspondence of a highly oriented and dense coverage of wide ZnTPP crystallites (*i. e.*, in samples grown at *T* = 105 °C). The reduced anisotropy signal observed at *T* = 130 °C, instead, is more likely related to the morphological degradation of the organic film at high temperature. Interestingly, the electronic properties of all the investigated samples were similar, with slight variations observed in the organic films grown at *T* = 105 °C and *T* = 130 °C, for instance, a change in the HOMO levels of the tetrapyrrolic ring, possibly related to the features observed in the optical anisotropy spectra. This aspect deserves a closer look in the future.

The preliminary results achieved so far will help us in finding the best strategy for growing organic films with an improved capability of protecting carbon-based electrodes from EC-induced deterioration phenomena. For instance, based on results of the morphological/optical investigation, we expect that ZnTPP films grown at *T* = 105 °C will show a good protection efficiency, since we speculate that the different crystal polymorphs present in the molecular film could ensure a uniform surface coverage, with few defect-sites.

The unique correlation we established between RA signal and morphology of the ZnTPP films provided a preliminary qualitative reference for a deeper monitoring of growth regimes and film quality, also in view of *in operando* experiments in different environmental conditions.

## Declaration of Competing Interest

The authors declare that they have no known competing financial interests or personal relationships that could have appeared to influence the work reported in this paper.

## Data availability

The data that has been used is confidential.

# Appendix A. Supplementary data

Supplementary data to this article can be found online at https://doi.org/10.1016/j.apsusc.2022.155729.

## References

[1] Z.D. Hao, X. Xu, H. Wang, J. Liu, H. Yan, Nano Br. Reports Rev. 13 (2018).
[2] Y. Liu, Z. Yang, J. Zhong, J. Li, R. Li, Y. Yu, F. Kang, ACS Nano 13 (2019) 11891–11900.
[3] D. Pavlov, P. Nikolov, J. Electrochem. Soc. 159 (2012) A1215 –A1225.
[4] W. Zhang, H. Lin, H. Lu, D. Liu, J. Yin, Z. Lin, J. Mater. Chem. A 3 (2015) 4399–4404.
[5] R. Yivlialin, G. Bussetti, L. Duò, F. Yu, M. Galbiati, L. Camilli, Langmuir 34 (2018).
[6] J. Xiang, P. Ding, H. Zhang, X. Wu, J. Chen, Y. Yang, J. Power Sources 241 (2013) 150–158.
[7] A. Banerjee, B. Ziv, Y. Shilina, E. Levi, S. Luski, D. Aurbach, A.C.S. Appl, Mater. Interfaces 9 (2017) 3634–3643.
[8] Z.W. Chang, J.J. Xu, Q.C. Liu, L. Li, X.B. Zhang, Adv. Energy Mater. 5 (2015).
[9] D.M. Itkis, D.A. Semenenko, E.Y. Kataev, A.I. Belova, V.S. Neudachina, A. P. Sirotina, M. Hävecker, D. Teschner, A. Knop-Gericke, P. Dudin, A. Barinov, E. A. Goodilin, Y. Shao-Horn, L.V. Yashina, Nano Lett. 13 (2013) 4697 –4701.
[10] G. Bussetti, R. Yivlialin, D. Alliata, A. Li Bassi, C. Castiglioni, M. Tommasini, C. S. Casari, M. Passoni, P. Biagioni, F. Ciccacci, L. Duò, J. Phys. Chem. C 120 (2016).
[11] R. Yivlialin, G. Bussetti, L. Magagnin, F. Ciccacci, L. Duò, Phys. Chem. Chem. Phys. 19 (2017).
[12] S. De Rosa, P. Branchini, R. Yivlialin, L. Duò, G. Bussetti, L. Tortora, ACS Appl. Nano Mater. 3 (2020).
[13] M.S. Jagadeesh, G. Bussetti, A. Calloni, R. Yivlialin, L. Brambilla, A. Accogli, E. Gibertini, D. Alliata, C. Goletti, F. Ciccacci, L. Magagnin, C. Castiglioni, L. Duò, J. Phys. Chem. C 123 (2019).
[14] F. Yu, L. Du, G. Zhang, F. Su, W. Wang, S. Sun, Adv. Funct. Mater. (2019).
[15] D. Hötger, M. Etzkorn, C. Morchutt, B. Wurster, J. Dreiser, S. Stepanow, D. Grumelli, R. Gutzler, K. Kern, Phys. Chem. Chem. Phys. 21 (2019) 2587 –2594.
[16] M. Penconi, R. Yivlialin, G. Bussetti, L. Duò, A. Bossi, A. Orbelli Biroli, Appl. Surf. Sci. 507 (2020).
[17] R. Yivlialin, G. Bussetti, M. Penconi, A. Bossi, F. Ciccacci, M. Finazzi, L. Duò, ACS Appl. Mater. Interfaces 9 (2017) 4100 –4105.
[18] A. Bossi, M. Penconi, R. Yivlialin, L. Duò, G. Bussetti, Encycl. Interfacial Chem. Surf. Sci Electrochem. (2018) 107 –118.
[19] T.B.T. To, F.D.A. Aarão Reis, Surfaces 5 (2022) 251 –264.
[20] G. Bussetti, L. Ferraro, A. Bossi, M. Campione, L. Duò, F. Ciccacci, Eur. Phys. J. Plus 136 (2021) 421.
[21] C. Castillo, R.A. Vazquez-Nava, B.S. Mendoza, Phys. Status Solidi C Conf. (2003) 2971–2975.
[22] B.S. Mendoza, R.A. Vázquez-Nava, Phys. Rev. B - Condens. Matter Mater. Phys. 72 (2005).
[23] C. Filoni, L. Duò, F. Ciccacci, A. Li Bassi, A. Bossi, M. Campione, G. Capitani, I. Denti, M. Tommasini, C. Castiglioni, S. De Rosa, L. Tortora, G. Bussetti, ChemNanoMat 6 (2020) 567–575.
[24] G. Berti, A. Calloni, A. Brambilla, G. Bussetti, L. Duò, F. Ciccacci, Rev. Sci. Instrum. 85 (2014) 73901.
[25] G. Bussetti, A. Calloni, M. Celeri, R. Yivlialin, M. Finazzi, F. Bottegoni, L. Duò, F. Ciccacci, Appl. Surf. Sci. 390 (2016) 856 –862.
[26] G. Bussetti, M. Campione, L. Ferraro, L. Raimondo, B. Bonanni, C. Goletti, M. Palummo, C. Hogan, L. Duò, M. Finazzi, A. Sassella, J. Phys. Chem. C 118 (2014) 15649–15655.
[27] G. Bussetti, M. Campione, L. Raimondo, R. Yivlialin, M. Finazzi, F. Ciccacci, A. Sassella, L. Duò, Cryst. Res. Technol. (2014) 581 –586.
[28] H.S. He, Acta Crystallogr Sect. E Struct. Reports Online 63 (2007) 976 –977.
[29] C. Goletti, R. Paolesse, E. Dalcanale, T. Berzina, C. Di Natale, G. Bussetti, P. Chiaradia, A. Froiio, L. Cristofolini, M. Costa, A. D`Amico, Langmuir 18 (2002) 6881–6886.
[30] N. Cecil, M. Magdaong, M. Taniguchi, J.R. Diers, D.M. Niedzwiedzki, C. Kirmaier, J.S. Lindsey, D.F. Bocian, D. Holten, J. Phys. Chem 2020 (2020) 7776 –7794.
[31] S. Rangan, S. Katalinic, R. Thorpe, R.A. Bartynski, J. Rochford, E. Galoppini, J. Phys. Chem. C 114 (2010) 1139 –1147.